

Effect of manganese (0%, 0.5% and 1%) doping on the optical and crystal properties of Barium Titanate (BaTiO_3) synthesised by Chemical Solution Deposition (CSD) method

Aep Setiawan^{1,2*}, *Iman Noor*^{2,3}, *Irmansyah*⁴, *Ridwan Siskandar*¹, *Erry Dwi Kurniawan*⁵, *Muhammad Mahyiddin Ramli*⁶, and *Irzaman*^{3*}

¹Computer Engineering Technology, IPB University Vocational School, Bogor, Indonesia

²Doctoral Program, Department of Physics, Faculty of Mathematics and Natural Sciences, IPB University, Bogor, Indonesia

³Physics Education Study Program, Faculty of Mathematics and Natural Sciences, Indraprasta PGRI University, Jakarta, Indonesia

⁴Department of Physics, Faculty of Mathematics and Natural Sciences, IPB University, Bogor, Indonesia

⁵Research Centre of Electronics, National Research and Innovation Agency (BRIN), Cisitu Bandung, Indonesia

⁶Institute of Nano Electronic Engineering, Universiti Malaysia Perlis, Kangar, Perlis 01000, Malaysia

Abstract. This study aims to investigate the effect of Manganese (Mn) ion addition on the optical and ferroelectric properties of Barium Titanate (BaTiO_3) materials synthesised by the Chemical Solution Deposition (CSD) method. The variations of the Mn dopant used are 0%, 0.5%, and 1% atoms to BaTiO_3 . This study used a UV-Vis spectrophotometer to determine the band gap energy via the Kubelka-Munk method, and employed X-ray diffraction (XRD) to determine the lattice parameters, spontaneous polarisation, and dipole moment. The lattice parameters were found to change significantly with Mn incorporation, with BaTiO_3 exhibiting $a = 4.22 \text{ \AA}$ and $c = 4.61 \text{ \AA}$, $\text{BaTi}_{0.995}\text{Mn}_{0.005}\text{O}_3$ showing increased values of $a = 5.48 \text{ \AA}$ and $c = 5.52 \text{ \AA}$, and $\text{BaTi}_{0.99}\text{Mn}_{0.01}\text{O}_3$ having $a = 5.13 \text{ \AA}$ and $c = 5.45 \text{ \AA}$. The value of spontaneous polarisation decreased slightly from 0.1826 C/m^2 to 0.1815 C/m^2 at 1% Mn doping, indicating a reduction in dipole-domain regularity due to Mn ion substitution at the Ti site. These results show that Mn doping can effectively modify the electronic and ferroelectric properties of BaTiO_3 , potentially improving material performance for capacitor and optoelectronic sensor applications.

* Corresponding author: aepsetiawan@apps.ipb.ac.id, irzaman@apps.ipb.ac.id

1 Introduction

Perovskite-based materials, such as Barium Titanate (BaTiO_3), have attracted significant attention in materials science due to their unique ferroelectric, piezoelectric, and optoelectric properties [1]. Its crystal structure is stable at room temperature, and its ability to withstand spontaneous polarisation makes it a key ingredient in a wide range of applications, including multilayer capacitors, actuators, pressure sensors, non-volatile memory, and photocatalysts [2-5]. However, the optical and electrical properties of BaTiO_3 can be modified by partial replacement of transition-metal ions at the Ti^{4+} site, thereby adjusting the dielectric constant and the bandgap energy [6].

One effective approach to improving BaTiO_3 performance is to dope it with transition metals, such as Fe, Co, and Mn. These ions play an important role in controlling oxygen defects, lattice distortion, and the formation of new energy levels within the band gaps [7]. Among these dopants, Manganese (Mn) can act as a donor or acceptor depending on oxidation conditions and the location of substitution in the perovskite lattice [8]. The incorporation of Mn into BaTiO_3 increases resistivity, enhances thermal stability, and modifies ferroelectric characteristics by generating internal fields resulting from $\text{Mn}^{2+}/\text{Mn}^{3+}$ substitution at the Ti^{4+} site [9].

Some studies suggest that Mn doping can significantly alter the band gap energy (E_g). For example, reported that the addition of Mn to BaTiO_3 can increase E_g by up to 3.8 eV due to the local-field effect of the d-electron Mn on the oxygen valence band [10]. The increased Mn doping can widen the band gap to some extent before saturation occurs due to increased oxygen defects [9]. In addition, the influence of dopant on lattice parameters (a and c) causes changes in the tetragonal structure to pseudo-cubic at high doping rates [5].

The synthesis method also plays an important role in determining the homogeneity and phase quality of $\text{BaTiO}_3:\text{Mn}$. In contrast to the solid-state method, which produces large, heterogeneous granules, the Chemical Solution Deposition (CSD) method can produce thin layers with smooth morphology, high purity, and uniform dopant distribution [9]. Another advantage of this method is its ability to produce stable crystal structures at lower sintering temperatures and thin films with high optical stability [10].

Based on this background, this study focuses on the effect of Mn doping (0, 0.5, and 1%) on the optical and ferroelectric properties of BaTiO_3 synthesised by the CSD method. The analysis examined changes in energy gap (UV-Vis), lattice parameters and crystal structure (XRD), as well as dipole moment and spontaneous polarisation [11]. This research aims to advance understanding of the structural-property modification mechanisms in the $\text{BaTi}_{1-x}\text{Mn}_x\text{O}_3$ system and to create opportunities for developing multifunctional ferroelectric materials for next-generation energy and sensor applications.

2 Experimental method

2.1 Synthesis

The main ingredients used are Barium Acetate powder [$\text{Ba}(\text{CH}_3\text{COO})_2$, 99%], Titanium Isopropoxide [$\text{Ti}(\text{C}_{12}\text{O}_4\text{H}_{28})$, 97%], and Manganese Acetate [$\text{Mn}(\text{CH}_3\text{COO})_2$, 99.99%] as the source of Mn ions. The synthesis process uses the Chemical Solution Deposition (CSD) method. First, all precursors were dissolved in a solvent of 2-methoxyethanol [$(\text{C}_3\text{H}_8\text{O}_2)$, 99.8%], then stirred magnetically in a stirrer on a hop plate for 2 hours at 40 °C with a rotation speed of 500 RPM. The solution is then filtered using a PVDF filter (0.45 micrometres) to make it more homogeneous. The next process is the spin coating process. The solution is dripped onto a silicone substrate placed on a spin coater, then rotated at 3000 RPM for 30

seconds, with up to 3 drops. After spin coating, the material undergoes annealing. Before the heating process begins, the film sample is placed in a crucible to prevent contamination. The first heating stage involves a temperature increase of 1.67 °C/min for 8 hours. After reaching 550 °C, the furnace maintains this temperature for another 8 hours. The final stage of this process is a temperature reduction back to room temperature over approximately 13 hours.

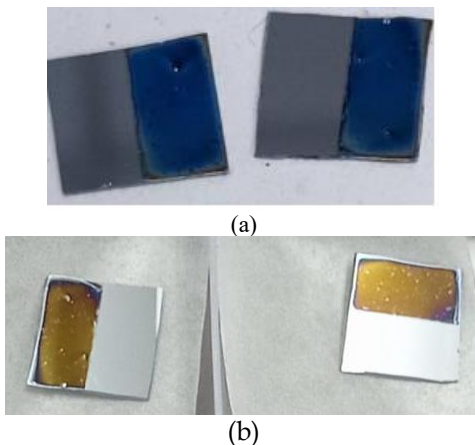


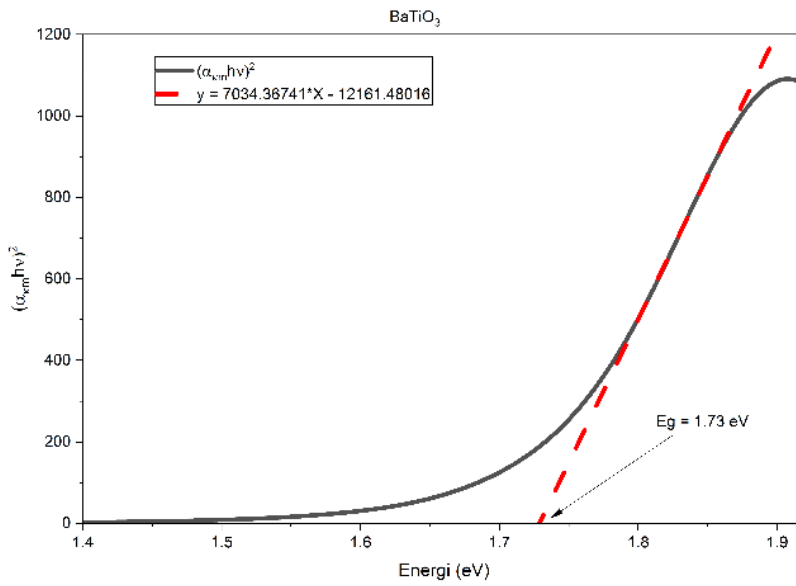
Fig. 1. (a) BST samples that have been in the furnace, (b) BST sample that has been spin-coated

2.2 Characterisations

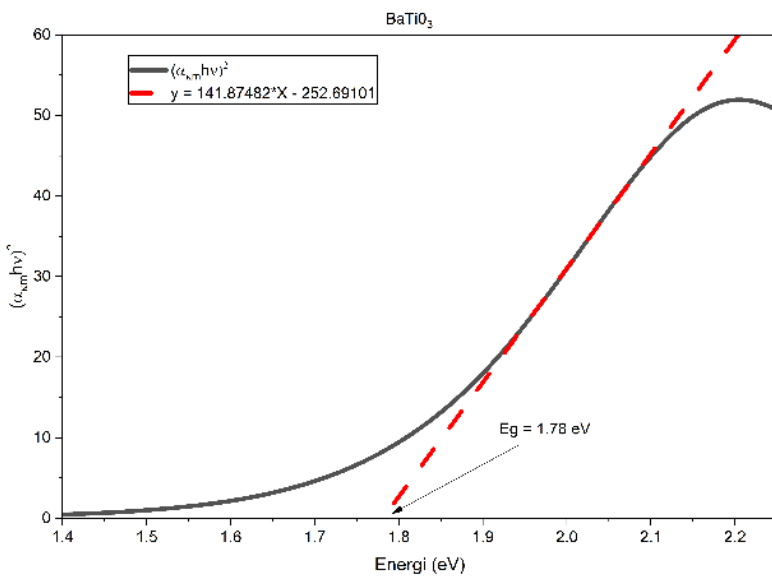
The UV–Vis spectroscopy measurement was performed in reflectance mode. Determines the band gap energy (E_g) using Plot Touch method based on the $(\alpha h\nu)^2$ vs. $h\nu$ plot. X-ray diffraction (XRD) determines the lattice parameters (a and c). It enables the calculation of the dipole moment (μ) and spontaneous polarisation (P_s) based on the tetragonal crystal structure parameters of $BaTiO_3$.

3 Result and discussion

Figures 2 to 4 show the results of processing the reflectance spectrum data analyzed using Origin software. The analysis was performed by converting the reflectance data into optical absorption functions using the Kubelka–Munk method. Next, extrapolation of the linear portion of the curve from the Kubelka–Munk graph was used to calculate the band gap energy value.

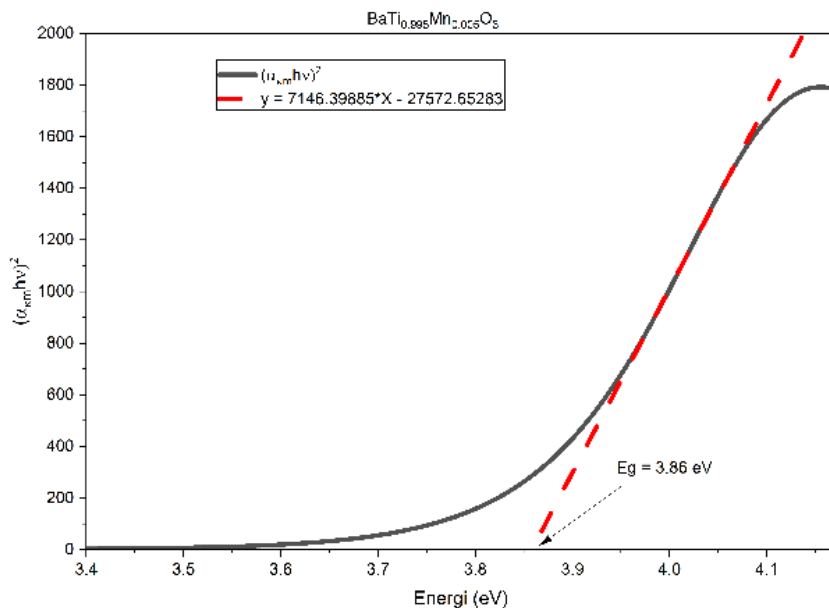


(a)

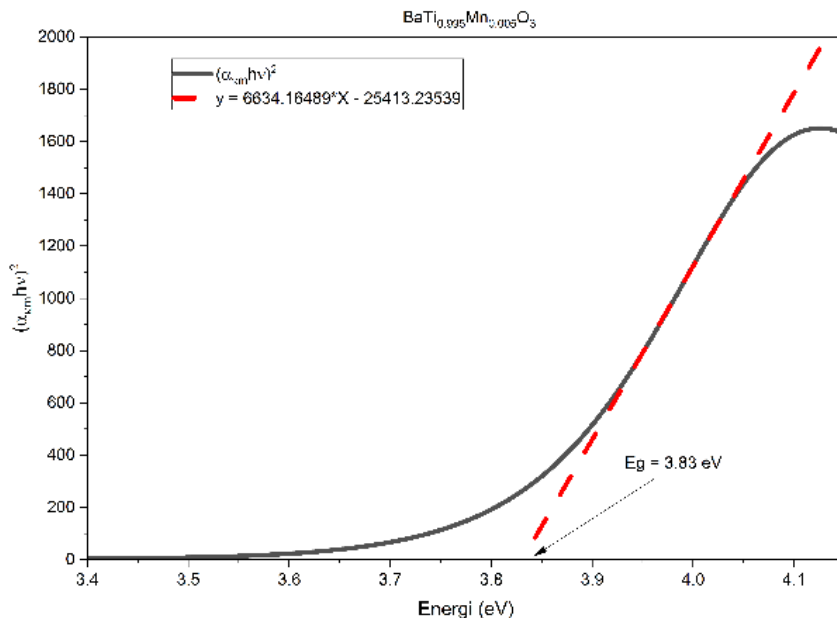


(b)

Fig. 2. Tauc Plot results using Kubelka–Munk method for energy gap determination (a) and (b) the energy gap value for BaTiO₃



(a)



(b)

Fig. 3. Tauc Plot results using Kubelka–Munk method for energy gap determination (a) and (b) the energy gap value for $\text{BaTi}_{0.995}\text{Mn}_{0.005}\text{O}_3$

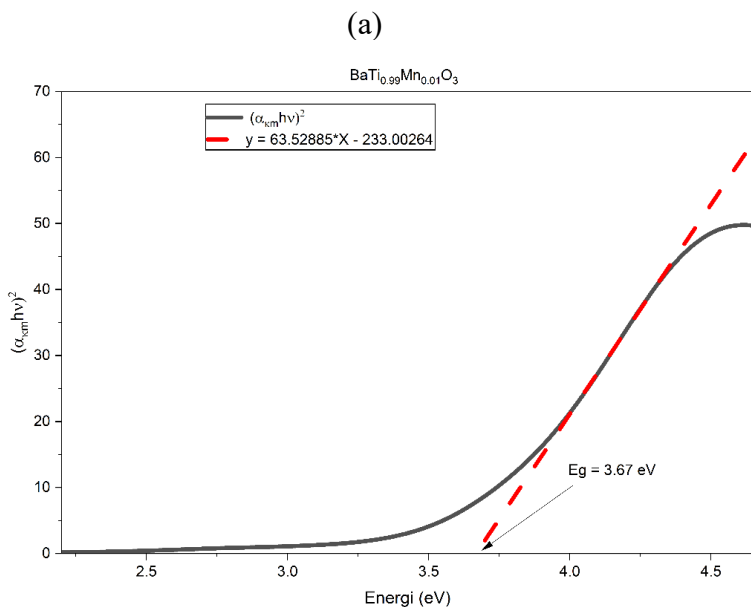
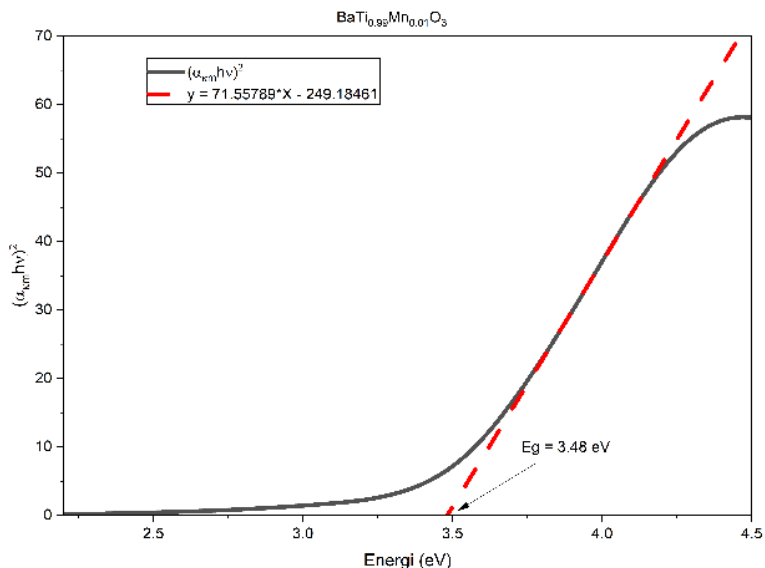


Fig. 4. Tauc Plot results using Kubelka–Munk method for energy gap determination (a) and (b) BaTi_{0.99}Mn_{0.01}O₃

Table 1. Energy gap value

Compound	Energy Gap Value		Energy Gap Literature [5]
	Repetition 1	Repetition 2	
BaTiO ₃	1.73 eV	1.78 eV	3.00 – 3.50 eV.
BaTi _{0.995} Mn _{0.005} O ₃	3.86 eV	3.83 eV	
BaTi _{0.99} Mn _{0.01} O ₃	3.48 eV	3.67 eV	

Table 1 presents the band gap energy values obtained from the Kubelka–Munk method. Pure BaTiO₃ has an E_g value of 1.73–1.78 eV, which is smaller than the literature value (3.0–3.5 eV) [5]. After the addition of 0.5% and 1% Mn dopant, the E_g values increased to 3.83–3.86 eV and 3.48–3.67 eV, respectively. The filling of the Mn d-level increases the band gap by widening the gap between the valence and conduction bands. However, at 1% doping, the decrease in E_g occurs again due to increased oxygen defects, creating energy levels within the band gaps that effectively shrink E_g. This behaviour is consistent with previous reports on the BaTiO₃:Mn system by R. P. Rini (2019), where an increase in Mn levels can amplify direct optical transitions to some extent before saturation.

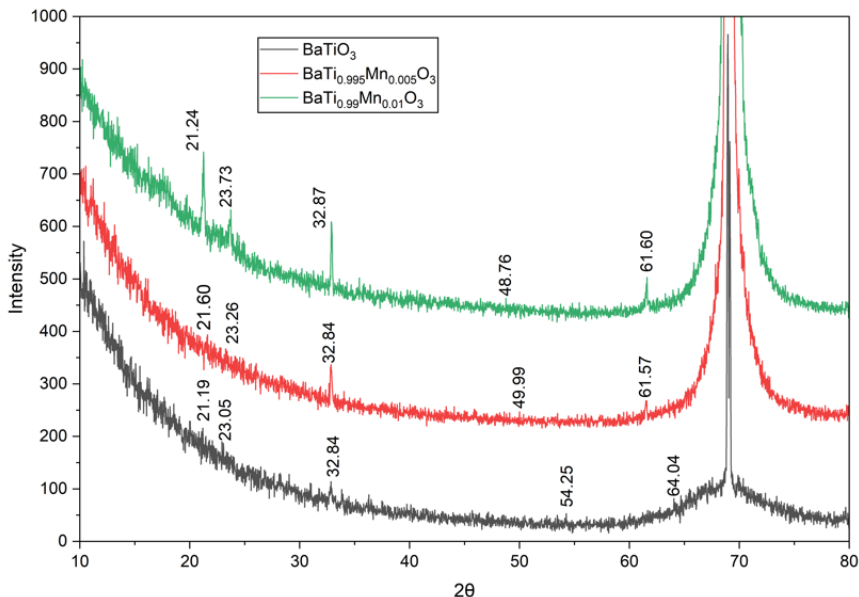


Fig. 5. XRD Results for BaTiO₃, BaTi_{0.995}Mn_{0.005}O₃, and BaTi_{0.99}Mn_{0.01}O₃

The XRD pattern shown shows a comparison between pure BaTiO₃ and Mn-doped BaTiO₃ samples at two different concentrations (BaTi_{0.995}Mn_{0.005}O₃ and BaTi_{0.99}Mn_{0.01}O₃). All samples showed diffraction peaks typical of the BaTiO₃ perovskite structure, indicating that Mn doping does not alter the main crystalline phase. However, the intensity and position of some peaks have changed slightly. A small change in this 2θ position usually indicates a lattice distortion or a change in lattice parameters due to the entry of Mn ions into the structure of BaTiO₃.

Peaks around 2θ ≈ 70° appear to increase in intensity as Mn concentration increases, suggesting a change in texture or preferred crystal orientation. The graph indicates successful Mn doping into the BaTiO₃ structure without the formation of a significant secondary phase.

Table 2. BaTiO₃ Dipole Moment Parameter Values

Compound	Lattice Parameter		References [12]		Dipole Moment (C.m)	Reference Dipol Moment (C.m) [13]
	a (Å)	c (Å)	a (Å)	c (Å)		
BaTiO ₃	4.22	4.61	3.99	4.04	1.175 x 10 ⁻²⁹	1.140 x 10 ⁻²⁹
BaTi _{0.995} Mn _{0.005} O ₃	5.48	5.52	-	-	1.154 x 10 ⁻²⁹	-
BaTi _{0.99} Mn _{0.01} O ₃	5.13	5.45	-	-	1.168 x 10 ⁻²⁹	-

Table 2 illustrates how the grid parameters changed based on the XRD data. While 0.5% Mn-doped BaTiO₃ displays higher values of $a = 5.48 \text{ \AA}$ and $c = 5.52 \text{ \AA}$, pure BaTiO₃ displays lattice parameters of $a = 4.22 \text{ \AA}$ and $c = 4.61 \text{ \AA}$. The substitution of Mn²⁺ ions ($r = 0.67 \text{ \AA}$) for Ti⁴⁺ ions ($r = 0.605 \text{ \AA}$) and Ba²⁺ ($r = 1.35 \text{ \AA}$) results in a small displacement of the tetragonal structure, which suggests lattice strain. The shift of Ti ions in the TiO₆ octahedron, which is directly correlated with the strength of the spontaneous polarization and local dipole moment, may be impacted by this distortion.

Table 3. Spontaneous Polarisation calculation results

Compound	Spontaneous Polarisation (C/m ²)	Reference Spontaneous Polarisation Ba _{0.625} Sr _{0.375} TiO ₃ (C/m ²) [13]	Reference Spontaneous Polarisation of BaTiO ₃ (C/m ²) [14]	Reference Spontaneous Polarisation of BaTiO ₃ (C/m ²) [15]
BaTiO ₃	0.182640424	0.18249	0.24	0.17
BaTi _{0.995} Mn _{0.005} O ₃	0.179346441	-	-	-
BaTi _{0.99} Mn _{0.01} O ₃	0.18151277	-	-	-

The computed spontaneous polarization (Ps) is shown in Table 3. At 0.5% and 1% Mn doping, the μ value of pure BaTiO₃, which was $1.175 \times 10^{-20} \text{ C}\cdot\text{m}$, slightly dropped to $1.154 \times 10^{-29} \text{ C}\cdot\text{m}$ and $1.168 \times 10^{-20} \text{ C}\cdot\text{m}$. As the Mn dopant increases, spontaneous polarization similarly reduces, going from 0.1826 C/m^2 to 0.1815 C/m^2 . This slight drop supports the idea that the Mn ion may function as an electron acceptor, preventing the Ti⁴⁺ ions from shifting and weakening the dipole local field. However, the material's continued high Ps value indicates that it still has strong, stable ferroelectric characteristics, which makes it a viable option for high-temperature piezoelectric sensors and high-energy capacitors.

4 Conclusion

The optical characteristics and structural features of BaTiO₃ are altered by Mn doping. The band gap energy rises at 0.5% Mn doping and slightly falls at 1% Mn doping; however, due to the poor accuracy of the data, this pattern needs more confirmation. The lattice parameters exhibit a tendency to expand, associated with the possible substitution of Mn ions into the BaTiO₃ lattice. Furthermore, the dipole moment and polarization values estimated from the structural parameters show a slight decrease, indicating a change in the crystal structure configuration due to Mn doping. Overall, the findings show that Mn doping affects BaTiO₃'s optical characteristics and structural factors, enabling the material's features to be fine-tuned within measurement accuracy bounds.

References

1. S. Mukherjee, D. Phuyal, C.U. Segre, S. Das, T Edvinsson, H. Rensmo, Structure and electronic effects from Mn and Nb Co-doping for low band gap BaTiO₃ ferroelectrics. *J. Phys. Chem. C*. **125**, 14910-14923 (2021). <https://doi.org/10.1021/acs.jpcc.1c02539>
2. I. Olaniyan, A. Blázquez Martínez, V.V. Hevelke, S. Wiesner, R. Wu, T.L. Phan, R. Cours, N. Cherkashin, S. Schamm-Chardon, D.-J. Kim, C. Dubourdieu, Optically induced irreversible ferroelastic and ferroelectric switching in epitaxial BaTiO₃ films on silicon. *ACS Nano*. **19**, 37534-37543 (2025). <https://doi.org/10.1021/acs.nano.5c05309>
3. A.R. Shenoy, M.M.N. Vijayalekshmi, D. Raj, A. Ani, P. Varghese, Exploring structural and optical properties of nanoparticles of Barium Titanate and Iron doped Barium

- Titanate and their potential application in antibacterial activity. *Current Physical Chemistry*. **15**, 1 (2025). <https://doi.org/10.2174/0118779468337862240930190440>
4. Irzaman, M. Darul, M. Rahmani, A.M. Rukyati, Samsidar, Nurhidayah, F. Deswardani, M. Peslinof, R.P. Jenie, J. Iskandar, Y. Wahyuni, K. Priandana, R. Siskandar, Design and fabrication of photovoltaics based on MFS (Ag/BaTiO₃/silicon p-type) structure. *Mater. Sci. Energy Technol.* **7**, 29–34 (2024). [doi: 10.1016/j.mset.2023.06.002](https://doi.org/10.1016/j.mset.2023.06.002)
 5. C.N. Eze, A.I. Onyia, M.N. Nnabuchi, A study of chemically deposited barium titanate (BaTiO₃) thin films doped with natural dyes and their photovoltaic applications. **11**, 6 (2023).
 6. X. Tong, Y-H. Lin, S. Zhang, Y Wang, C-W. Nan, Preparation of Mn-doped BaTiO₃ nanoparticles and their magnetic properties. *J. Appl. Phys.* **104**, 066108 (2008). <https://doi.org/10.1063/1.2973202>
 7. S. Landi, I.R. Segundo, E. Freitas, M. Vasilevskiy, J. Carneiro, C. Jos, Use and misuse of the Kubelka-Munk function to obtain the band gap energy from diffuse reflectance measurements. *Solid State Communications*. **341**, 1–7,(2022). <https://doi.org/10.1016/j.ssc.2021.114573>
 8. K. Madhan, R. Thiyagarajan, C. Jagadeeshwaran, A.P.B. Selvadurai, V. Pazhanivelu, K. Aravinth, W. Yang, R. Murugaraj, Investigations on the phase transition of Mn-doped BaTiO₃ multifunctional ferroelectric ceramics through Raman , dielectric , and magnetic studies. *J. Sol-Gel Sci. Technol.* **88**, 584–592 (2018). <https://doi.org/10.1007/s10971-018-4835-3>
 9. X. Niu, X. Jian, X. Chen, H. Li, W. Liang, Y. Yao, T. Tao, B. Liang, S-G. Lu, Enhanced electrocaloric effect at room temperature in Mn²⁺ doped lead-free (BaSr) TiO₃ ceramics via a direct measurement. *J. Adv. Ceram.* **10**, 482–492 (2021). <https://doi.org/10.1007/s40145-020-0450-1>
 10. K. Bakken, A. Bank, M. Einarsrud, J. Glaum, Mechanisms for texture in BaTiO₃ thin films from aqueous chemical solution deposition. *J. Sol-Gel Sci. Technol.* 562–572 (2020). <https://doi.org/10.1007/s10971-020-05356-2>
 11. A. Setiawan, E.K. Palupi, R. Umam, H. Alatas, Irzaman, Optical characterization of Ba_{0.5}Sr_{0.5}TiO₃ material grown on a p-type silicon substrate (111) doped niobium oxide and chlorophyll. *Ferroelectrics*. **568**, 62–70 (2020). [doi: 10.1080/00150193.2020.1735893](https://doi.org/10.1080/00150193.2020.1735893)
 12. H.E. Swanson, R.K. Fuyat, G.M. Ugrinic, Barium titanate, BaTiO₃ (tetragonal). In *Standard X-ray Diffraction Powder Patterns*. Vol. III: Data for 34 Inorganic Substances (NBS Circular 539, pp. 44–45). (National Bureau of Standards, Washington DC, 1954)
 13. I.R. Nurzaman, Perhitungan polarisasi spontan pada bahan ferroelektrik Ba_xSr_{1-x}TiO₃ dengan variasi Sr. Bachelor Thesis, Institut Pertanian Bogor, Bogor, Indonesia (2015)
 14. J. Dionot, G. Geneste, C. Mathieu, N. Barrett, Surface polarization, rumpling, and domain ordering of strained ultrathin BaTiO₃ (001) films with in-plane and out-of-plane polarization. *Physical Review*. **90**, 014107 (2014). <https://doi.org/10.1103/PhysRevB.90.014107>
 15. K. Uchino, Fellow, Electrostrictive and Piezoelectric Effects in Relaxor Ferroelectrics: Historical Background. *IEEE Trans. Ultrason. Ferroelectr. Freq. Control*. **69**, 11 (2022). <https://doi.org/10.1109/TUFFC.2022.3165002>